A Graph-based Approach with Simulated Traffic Dynamics for the Analysis of Transportation Resilience in Smart Cities

Elise Henry, Angelo Furno, Nour-Eddin El Faouzi

Transportation Research Record

A Graph-based Approach with Simulated Traffic Dynamics for the Analysis of Transportation Resilience in Smart Cities

--Manuscript Draft--

Full Title:	A Graph-based Approach with Simulated Traffic Dynamics for the Analysis of Transportation Resilience in Smart Cities
Manuscript Number:	19-05484R1
Article Type:	Presentation Only
Order of Authors:	Elise Henry, Master Student
	Angelo Furno
	Nour-Eddin El Faouzi

A Graph-based Approach with Simulated Traffic Dynamics for the Analysis of Transportation Resilience in Smart Cities

Submission Date: November, 15th 2018

Elise Henry[1],
[1] Univ. Lyon, IFSTTAR, ENTPE, LICIT UMR_T9401, F-69675, Lyon, France
elise.henry@ifsttar.fr

Angelo Furno[1],
[1] Univ. Lyon, IFSTTAR, ENTPE, LICIT UMR_T9401, F-69675, Lyon, France
angelo.furno@ifsttar.fr

Nour-Eddin El Faouzi[1,2]
[1] Univ. Lyon, IFSTTAR, ENTPE, LICIT UMR_T9401, F-69675, Lyon, France
[2] Queensland University of Technology, STRC, Gardens Point Campus, 2 George Street, G.P.O. Box 2434, Brisbane, Queensland 4001, Australia.
nour-eddin.elfaouzi@ifsttar.fr

Submitted to the 98th Annual Meeting of the Transportation Research Board for publication and presentation

---

Word Count:

Number of words: 5706
Number of tables: 0 (250 words each)
Total: 5706

Abstract

Large urban areas are vital for the economic and social development of modern cities. The mobility in these areas strongly depends on a seamless and available multi-modal transport infrastructure network. Since many of these networks operates at capacity limits, any disruptions of a single edge can have negative effects on the mobility. Hence, modeling and quantifying the resilience of large-scale urban transport networks will allow cities guaranteeing higher quality of service, even in the presence of unpredictable disruptive events.

This paper aims to develop a new methodology linking together topological data with traffic dynamics for resilience analysis. To do so, we adopt a dynamic weighted graph approach where weights are generated according to prevailing traffic conditions. Weight-extended centrality measures are leveraged in order to capture the evolution of vulnerabilities. The paper also aims at studying the impact of area-wide disruptions, such as snow storms or floods, insufficiently explored in the literature. This is based on a stress testing approach. Our graph-based approach is also supported by other analyses performed in the paper by leveraging more traditional traffic indicators.

Results demonstrate the importance of both the spatial and temporal dimension in the assessment of transport network criticality, thus stressing the importance of jointly considering the topological properties and traffic dynamics in the study of transport resilience. Consequences of area-wide disruptions are also proved to be different with respect to single-link failures, therefore deserving a deeper characterization in the study of transport resilience.

Keywords: **Smart Transportation, Resilience, Stress Tests, Dynamic Graph**

1. INTRODUCTION

Infrastructural vulnerabilities and extreme events negatively affect the performance of transport networks. They have to be taken into account to improve transport resilience which is defined as "*the ability of a system to operate under variable and unexpected conditions without substantially compromising its planned performances*" [1]. Thanks to resilience, network performances could be quantified under normal conditions and when a disruptive event occurs.

Research in this field is fundamental from the perspectives of both transport authorities and travelers, since it can help the smooth operation of mobility services and support rescue operations as well. Nowadays, resilience is modeled and assessed either in a static way - mainly based on traffic network topological insights achieved by means of graph theory - or dynamically by means of simulations taking into account fairly realistic and time-varying traffic conditions. Structural and dynamical resilience analysis, often lead separately despite their complementary, are essential to a better understanding of network vulnerabilities. In addition, disturbances analysis has traditionally been focused on link disruptions whereas some events can impact entire areas [2].

For these reasons, the aim of this paper is to investigate novel solutions for resilience modeling and analyses, by trying to answer the following questions: how can we improve network resilience assessment by joining static, purely topological approaches to those based on traffic dynamics? How can we characterize and quantify, from the perspective of network resilience, the consequences stemming from disruptive events that affect entire areas of a city?

This work seeks therefore to advance state-of-the-art research in the field of resilience engineering by means of the following contributions: (1) we develop a methodology to integrate dynamic characteristics of the analyzed transport network into topological metrics that are traditionally static by means of an evolving, transport-appropriate, weighing. The obtained dynamically-weighted graph shall be able of grasping realistic and time-varying traffic-properties of the considered road network; (2) we assess the impact of area-wide disruptions by modeling, via stress tests and simulation tools, events that reduce network capacity on entire areas of the transport network, rather than considering single-link failures as done in most of the traditional approaches in resilience engineering [2]. Such an analysis aims to clearly highlight the importance of assessing area-wide disruptions in transport resilience studies; (3) we compare resilience metrics to a classical traffic-specific indicator, the macroscopic fundamental diagram (MFD) [3], which allows to characterize the performance of an entire area in terms of flow, speed and concentration.

The paper is organized as follow. Section 2 briefly surveys related work dealing with network resilience. Section 3 outlines the proposed methodology to construct a transport relevant weighing graph and the implementation of area-wide disturbances. Comparison between resilience metrics and traffic indicator is also presented at the end of the section. In Section 4, we present our case study and discuss the application of the proposed methodology to it. In Section 5, we discuss the main insights deriving from our case study and conclude our paper by also highlighting some research direction for future work.

2. LITERATURE REVIEW

2.1. Definition of resilience

Many definitions of resilience exist in the literature highlighting the lack of a universally accepted definition [4]. Since the introduction of this concept in the field of ecology [5], resilience has been studied in different domains. In communication networks, it is defined as *"the ability of the network to provide and maintain an acceptable level of service in the face of various faults and challenges to normal operation"* [6].

The most quoted definition is the one of Bruneau et al., [7] who breaks down the notion of resilience in three temporal phases: (1) *before perturbation*, corresponding to the notion of robustness,

(2) *during perturbation*, corresponding to the notion of reactivity, and (3) *after perturbation*, corresponding to the notion of recovery. Berckley et al. [8] extended the definition above by including a *feedback phase* corresponding to the notion of adaptability. In the field of transportation, Mattsson et al. [9] recently advocated the lack of adequate research on the topic, particularly with respect to the post-disaster phase. Since then, resilience has emerged as a vast domain of investigation, with a growing and active community. In this context, definitions, metrics and approaches stemming from other research fields and domains, such as telecommunications or computer systems and networks, are proving to be crucial in the transport domain as well [6, 10].

2.2. Approaches and metrics

Currently, the assessment of transport network resilience is led via two different major approaches: topological and dynamic. Combinations of both methods are rare but promising, based on the idea of joining graph theory with simulated or data-inferred traffic conditions. Shalaby et al. [11] and Gauthier et al. [12] compare public transport and road networks resilience quantified with both approaches. Preliminary results of [12] demonstrate the importance of this combination as topological approaches are traditionally unable to grasp the time-dependent aspects of resilience.

2.2.1. Topological Approaches

Topological approaches aim to quantify network resilience (especially according to the perspective of robustness) by looking at the connectivity properties of the network, by using graph theory. Transport networks are represented by an undirected or directed graph $G = (V, E)$, where edges (E) correspond to roads, and nodes (N) to intersections. Centrality measures are traditionally used to retrieve insights about in terms of network connectivity and accessibility. By studying various networks, with different topology, Derrible et al. [13] (28 different subway networks), Zhang et al. [14] (17 different networks from various fields) and Zhang et al. [15] (5 different kinds of network topologies) prove the importance of topological analysis to assess transport network resilience.

Although various centrality measures (closeness centrality, degree centrality, information centrality, etc.) exist, Betweenness Centrality (BC) [16] (Eq. 1) is among the preferred ones [15, 13, 12, 17, 18] to identify vulnerable links (i.e., those with highest BC values) in transport networks. To have a global view of network performances and characterize the impact of disturbed scenarios, Global Efficiency (GE) [19] (Eq. 2) has also been frequently employed [20, 21, 22, 23]. It quantifies how efficiently information (or any other kind of flow) is exchanged over the network. Via this metric, the effect of a disturbance can be quantified by comparing the variation of GE under normal and disrupted conditions. The formal definitions of BC and GE follow:

$$BC(e) = \sum_{j \neq i} \frac{\sigma_{ij}(e)}{\sigma_{ij}}, \tag{1}$$

$$GE(G) = \frac{1}{N(N-1)} \sum_{i \neq j} \frac{1}{l_{ij}}, \tag{2}$$

where $\sigma_{ij}(e)$ is the number of shortest paths from node i to node j crossing edge e, σ_{ij} is the total number of shortest paths from node i to node j, N is the number of graph nodes and l_{ij} is the length of the shortest path(s) from node i to node j.

Based on shortest paths computations, the weighting of edges allows to consider road characteristics information like the travel time, important in path choice, ensures that traffic dynamics are taken into account in centrality measures. Shortest paths correspond to the sequence of edges with minimal weights connecting the path origin to its destination.

Topological approaches are simplistic in the sense that they do not incorporate dynamic information about traffic nor time-varying characteristics of the network. Some recent attempts have been made to consider link time-dependent costs in the graph representation of the road network: links are weighted by free flow time in [12, 24, 25], temporal metrics for time-varying graphs have been also developed in [26]. In line with our work, Cheng et al. [27, 28] and Yoo et al. [29] propose extended definitions of the centrality indicators, proving the importance of including commuter flows and temporal delays (e.g., travel times) in the computation of the centrality measures.

2.2.2. Dynamic approaches

In this category fall all the approaches and metrics for resilience assessment that take into account the dynamics of the transport systems (traffic conditions) based on simulation or machine learning solutions for estimating future dynamics from historical data.

These approaches characterize resilience by taking into account actual or simulated traffic dynamics, using demand-sensitive indicators like links speed, queue length, road capacity or recovery time, as discussed in [30, 31].

Some metrics are based on comparisons of traffic conditions under normal and disturbed scenarios. In [32], the authors propose two metrics, *importance* (I), computing the importance of a link by disrupting it, and *exposure* (E), computing the expected increase in travel cost for a random link failure somewhere. Based on the increase of travel cost when a disruption occurs, they are among the most popular metrics that belong to the category of dynamic approaches [12, 11, 2].

Even though traditionally more accurate than topological solutions, dynamic approaches are limited in turns [12]. They tend to use heavy simulations which demand large execution time, by providing sometimes unreliable indications about resilience due to the hardness to model unpredictable situations, while real-time data based solutions are expected to be much more realistic.

Therefore, real-time traffic data should be included and exploited in graph-based models for resilience analysis. That will demand for novel solutions based on big data processing aiming at efficiently mining the traffic data for resilience analysis. In this paper, based on previous work [24, 12], we dynamically and efficiently compute centrality measures on weighted graphs, allowing to take traffic dynamics into account. To do so, we use data issued from simple simulation to feed our dynamic graphs with links travel time, because we do not have access to real-time data.

2.3. Stress testing

To model and quantify disruptions and their impact on a complex system, stress test methodology, which is a common practice in bank and nuclear industries, can be effectively considered and leveraged in the transport field, with relevant applications for resilience assessment [21, 12, 33]. A stress test is a *"quantitative assessment designed to evaluate the ability of a network to perform adequately during and after the occurrence of hazard events"* [33]. This allows to quantifying adverse impacts caused by disruptive scenarios. Comparing these cases to initial one give information about how the network is resilient, by regarding changes in metrics. To quantify resilience, road networks can be stressed by inducing a reduction in capacity over single links or multiple links contained in a given area of the network. A large majority of existing works have mainly quantified network resilience by assessing the impact of targeted or random removal of single or very few edges or nodes [11, 34, 35, 36, 37]. Recently, in our previous work [12], we have studied link capacity reduction rather than abrupt and complete link removal. Such an approach allows to better quantifying minor daily disruptive events that result in a reduction of road capacity (e.g., a decrease in the number of road lanes). Nonetheless, various disruptive events, like floods, snow-storms, fires, etc. may easily affect entire areas and cannot be modeled by the previous approach. Jenelius et al. [2] extended the importance and exposure metrics to take into account area-wide disruptions. In their study,

they completely prohibit the access to the links contained in the disturbed area, representing by grid-cells. They conclude that *"consequences are quite different from those of single link failures"*. In the evaluation section, we compare the impacts of link-failures and area-wide disruptions, with weighted centrality measures, by gradually reducing the capacity.

2.4. Macroscopic fundamental diagram

In this paper, we propose to use traffic indicators based on the fundamental diagram (FD) to characterize resilience. A FD characterizes road by relating three traffic variables whose formula stems from mechanic of fluid:

$$Q = V \cdot K_c = W \cdot (K_x - K_c) \tag{3}$$

where Q is the maximal capacity, V is the free flow speed, W the shock wave one, K_c represents the critical density and K_x the maximal one.

Introduced in late 2000s [3], the area-based FD, called Macroscopic Fundamental Diagram (MFD) relates the output flow and the number of vehicles in a large network, giving insights about the state of a zone over a road network. Already used in traffic control [38], could offer good opportunities in resilience analysis. Kim et al. [36] assess the resilience of a part of the transport network in the city of Seoul, South Korea, by using information issued from this traffic tool and by assessing some area properties as the outflow or the traffic density.

3. METHODOLOGY

3.1. Construction of a dynamic graph

By building on our previous work [12], we propose to adopt dynamic graphs modeling leveraging traffic conditions as time-varying weights associated to the links.

Road users tend to select their paths according to multiple variables, including travel time. However, we can reasonably state that paths are equally chosen by a user if they are perceived as "approximately" having the same total length, e.g., total travel time. The *"bounded rationality is neither the optimization nor the irrationality"* [39]. Bounded rationality corresponds to a choice done with flexible criterion with limited information processing resources and limited consideration of alternatives paths [40]. In order to improve the significance of the edge weights, we adopt a discretization process. This method provides the group of shortest paths, which represent the potential used roads, rather than the shortest one.

3.2. Weighting of the centrality measures

By leveraging the previously described dynamic, weighted, graph-based modeling of a road network, the BC of each edge, whose computation is based on the identification of the weighted shortest paths between each possible pairs of origin/destination via Dijkstra's algorithm [41], becomes a function of the time. In other words, the time-dependency of the BC metric permits better capturing the actual functioning of the transport network by taking into account additional key and dynamic features of the roads, like for instance the actual or simulated travel times, neglected in the basic unweighted definition of the BC metric. We therefore observe and analyze the evolution of BC over time as a consequence of the changes taking place in the weighted graph, whose edge weights evolve both because of regular traffic dynamics (i.e., travel time variations due to congestion phenomena or travel demand changes) and, possibly, as a consequence of unpredictable events (i.e., accidents, or even the stress tests we induce to model area-wide disruptions).

3.3. Area-wide disruption analysis via stress testing

To analyze the impact of area-wide disruptions with respect to single-link failures, we simulate disturbance over the links contained in the area, in two different ways. While, in the former case, disruption is applied simultaneously over all links, in the latter it is allocated successively to each link. Consecutive results are averaged. The methodology is based on stress testing, allowing to observe system functioning when it operates beyond its normal characteristics. Capacity is progressively reduced from 20% to 80% of the initial one.

3.4. Implementation of the methodology

3.4.1. Elaboration of a dynamic graph

To weight our graph and model traffic dynamics, we leverage a microscopic traffic simulator called SymuVia[1], developed by our research group. The simulator represents individual vehicles by computing transit times at each second, based on LWR (Lighthill-Whitham-Richards) model [42, 43]. The vehicles are distributed over the network, according to the traffic conditions at the moment the vehicle is generated. Before running a simulation, duration, origin-destination demands and limit speed per link have to be defined. The simulator allows for extracting speeds averaged by ten-minutes time stamps. Thus, by dividing link length by its simulated speed, we are able to weight edges by their travel time.

3.4.2. Weighting of the centrality measures

To discretize weights, we choose to group them according to their travel time. For the first interval, we consider the shortest link travel time t. All links whose length is in the range $[t, t + \alpha \cdot t]$ are considered equal and received the mean value as weight. The minimal value of the second interval is equal to $t + \alpha \cdot t$ and the maximal one is equal to $(t + \alpha \cdot t) + \alpha \cdot (t + \alpha \cdot t)$. Included links weight become the mean value of this second range. The process is iterated while the longest link travel time is not include in an interval. Then, we observe the effect of choosing α in the range $[0.1, 0.3]$. On the resulting graph, we apply *betweenness centrality* and *global efficiency*.

3.4.3. Stress testing

To simulate the capacity drop, we reduce progressively the speed limit according to the FD formula (Eq. 3). We use geographical zones defined by the French national institute of statistic and economic studies (INSEE) to analyze area-wide disruptions. The risk maps are in accordance with these areas and allows to allocate likely perturbations. Each area groups similar populations, implying that the size of the zone is relatively smaller especially in largely populated areas.

3.4.4. Traffic-specific indicator results

We choose to compare resilience metrics with macroscopic fundamental diagram. In our case, simulation set up are the following ones: maximal density is equal to 0.17 vehicles per meter and shock wave speed is about 5.88 meter per second. These characteristics do not change because there are defined per vehicle types (e.g. car, bus, trolley bus). The link speeds could be extracted from simulations. By summing the maximal density, k_x, of all links and their speeds, v and w, we obtain the maximal flow, q, and the critical density, k_c, with the same formula of the one used for the FD (Eq. 3). Therefore, we obtain information about a part or the entire network, according to the links taken into account.

[1] http://www.licit-lyon.eu/themes/realisations/plateformes/symuvia/

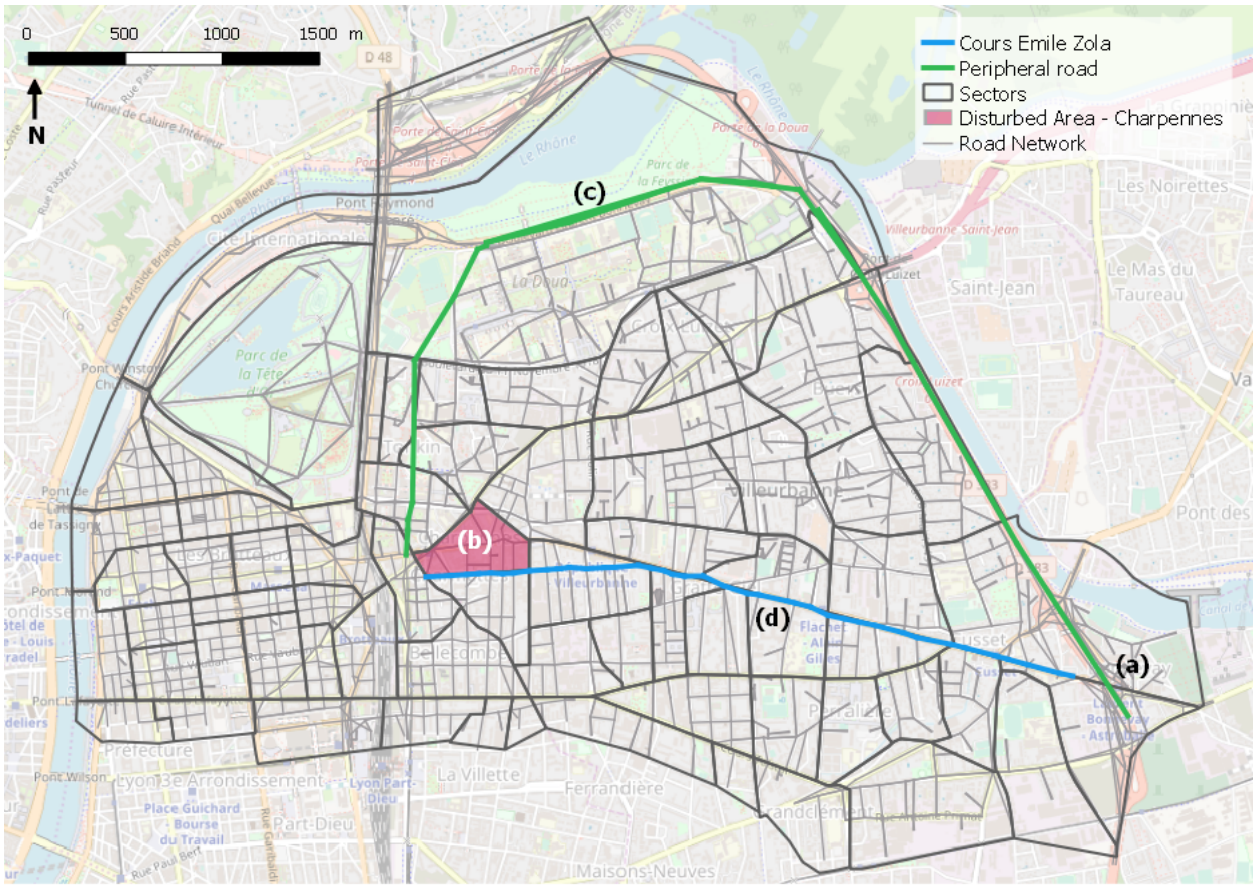

Figure 1: Case study - 3^{rd} and 6^{th} districts of Lyon and a part of Villeurbanne in France. (a) is the interchange, (b) the disturbed area "Charpennes" in section 4.4, (c) is the ring road and (d) the "Cours Emile Zola".

4. RESULTS

4.1. Case study

Our methodology has been evaluated on a real road network including the 3^{rd} and 6^{th} districts of Lyon and a part of the city of Villeurbanne in France. Such area allows to run simulation with an acceptable computation time and its size allows to observe vehicles movements. Moreover needed data, as the origin-destination matrix, are provided over this area. These three places have different social and economical characteristics. The 3^{rd} borough is the central business district of Lyon. It is also the most populated area of the city. The 6^{th} district has instead a dominant commercial function and a large population. These two parts of Lyon are the major tertiary centers of the city. Finally, Villeurbanne is a working-class city hosting one of the largest university of the region. The studied area comprises 1,774 nodes, 3,342 links and 68 sectors, represented as a directed graph coded in Python 3.6 by using the NetworkX library [44].

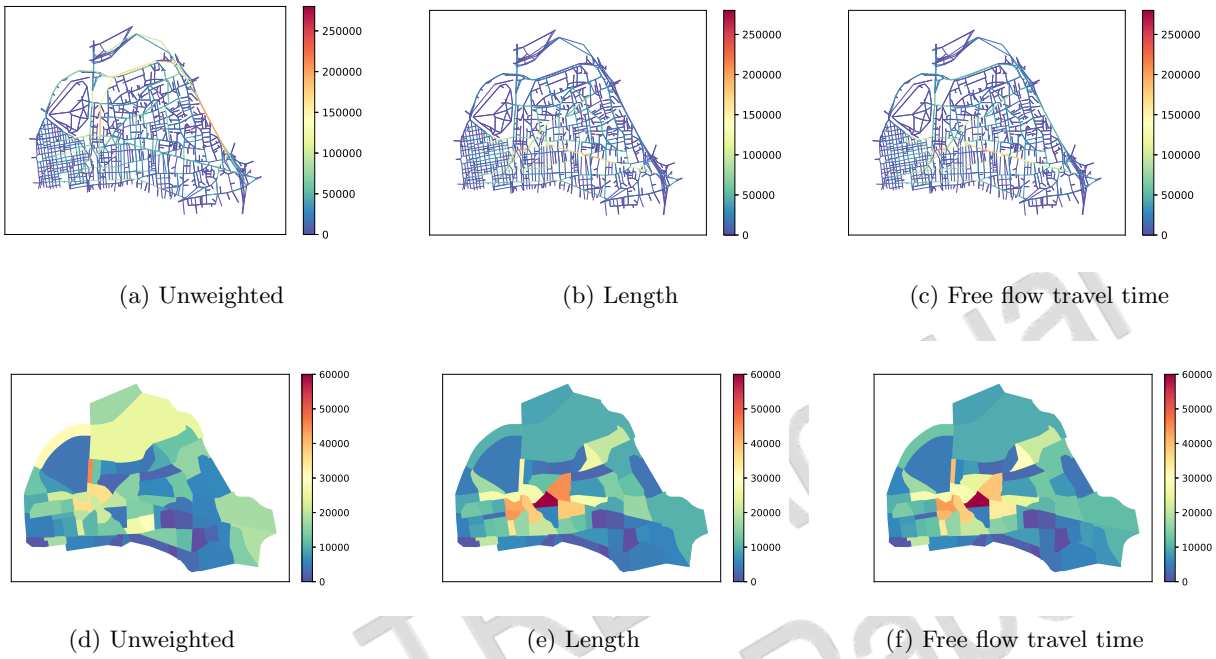

(a) Unweighted (b) Length (c) Free flow travel time

(d) Unweighted (e) Length (f) Free flow travel time

Figure 2: Comparison of unweighted, link length weighted and link travel time weighted edge BC over the studied area.

4.2. Weighting importance for BC

Weighting BC by free flow travel time is a first step towards merging static and dynamic approaches: in unweighted graphs, the length of the shortest paths is equal to the number of crossed hops. However, in realistic scenarios, the actual travel time of each road segment significantly impacts the path choice.

For the sake of simplicity, we present results per area. The zonal BC is equal to the average of the BC value associated to each link comprised within the given zone.

In Fig. 2a, we present the values of unweighted edge BC. The ring road, represented in green (Fig. 1c), possesses the highest BC due to the long length of the corresponding road segments. For instance, this is the shortest path because of the low number of crossed hops, to go from the interchange (Fig. 1a) to the red sector (Fig. 1b).

Taking length into account (Fig. 2b), the shortest path for same origin destination becomes “Cours Emile Zola” (Fig. 1d), with a distance of about 3km while the ring road one is approximately 6km. Due to the long length of the corresponding road segments, the ring road BC value approaches zero, which is not consistent with real world situation. Indeed, the ring road, even if longer in term of length, possesses a high limit speed, which has to be take into account in the shortest path research.

By weighting edges by their travel time, the ring road travel time benefit is considered. Fig. 2c shows an increase of ring road BC, due to its presence across some shortest paths.

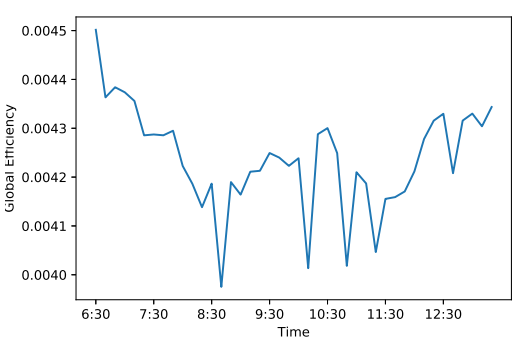

(a) Evolution of travel-time-weighted GE

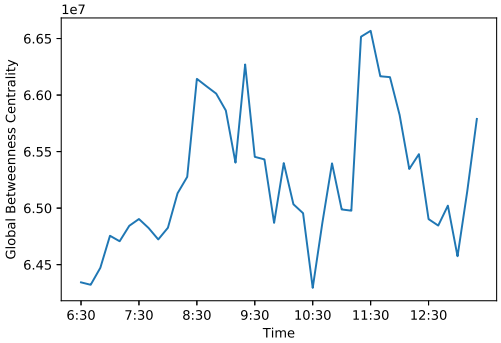

(b) Evolution of travel-time-weighted GBC

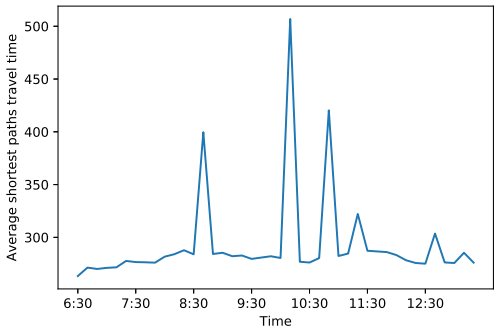

(c) Average shortest paths travel time

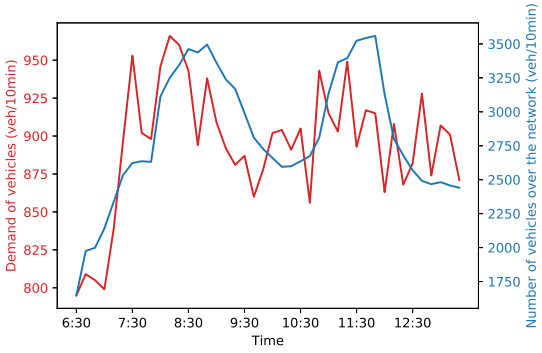

(d) Number of vehicles in the network

Figure 3: Evolution of the graph-based weighted metrics between 6:30am and 1:30pm.

4.3. Dynamic topological metrics

4.3.1. Evolution of network performances with "real" weights

In dynamic settings, weighted centrality measures evolve over time with traffic conditions. In our paper, the average travel times per ten minutes are derived from simulated scenario, performed from 6:30am to 1:30pm under normal conditions.

The results, graphically presented in Fig. 3, highlight a change in global performance over time, related to the evolution of vehicle number in response to the input demand, both reported in Fig. 3d. With the increase of vehicles present over the network, the GE (Fig. 3a) drops whereas the sum of the BC computed over all links, named in the following *global betweenness centrality* (GBC) rises. The change in performance means that the network is unbalanced, i.e. there are certain links traversed by more shortest paths (and therefore typically attracting more traffic) than other ones.

The appearance of traffic slowdowns increases the travel time of the traversed links. Thus, the value of travel time associated to the shortest paths at the successive time slots rises. The two following situations can occur: either vehicles continue traversing the same path, which will show, in the following time slots, a larger travel time because of congestion, or vehicles switch to a new path, which has a certain travel time, very likely larger than the one traversed during the previous time slot. The global increase of travel time associated to the different paths leads therefore to a decrease of GE (Fig. 3a), inversely proportional to the length (i.e., total travel time) of the shortest paths (Fig. 3c). This aspect is underscored at 8:40am, 10:10am and 11:20am. Interestingly, an opposite trend can be observed in relation to GBC: the spikes for GBC (Fig. 3b) can be explained

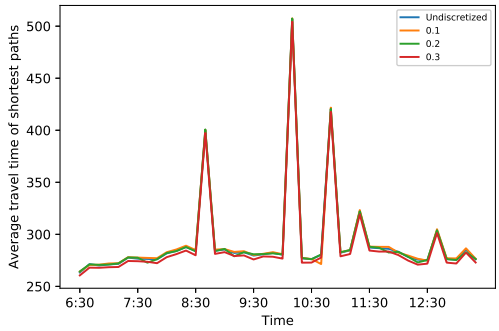

(a) Average shortest paths travel time

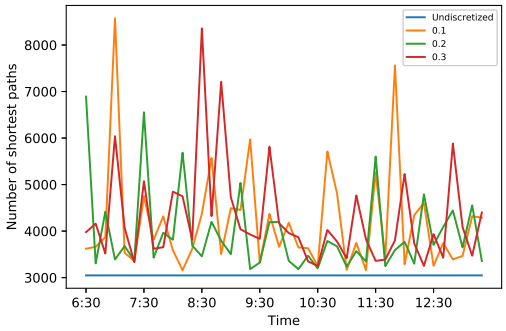

(b) Number of shortest paths

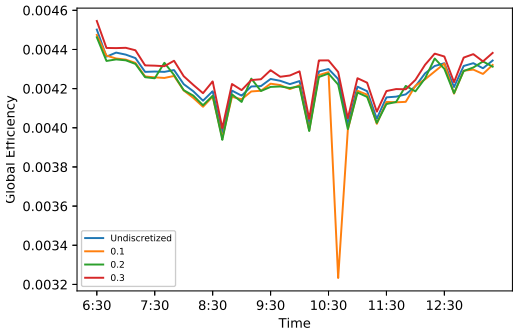

(c) Evolution of travel-time-weighted (TTW) GE

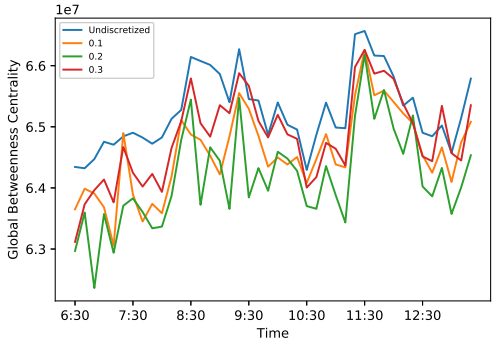

(d) Evolution of travel-time-weighted (TTW) GBC

Figure 4: Evolution of the graph-based weighted metrics between 6:30am and 1:30pm for discretized weights $[t, \alpha \cdot t]$ and different values of α under normal conditions.

by considering the relatively higher number of links traversed by a large number of shortest paths, meaning that the network becomes strongly unbalanced at demand peaks. In other words, more and more links become critical, raising the global GBC indicator.

4.3.2. Evolution of network performances with discretized weights

According to the users bounded rationality principle, the path choice has to be less demanding to obtain a resilience analysis relating to network usage rather than the use of the shortest path only. For that, we discretize edges weights in order to obtain a group of paths approximately equal (from the user's perspective) to the shortest one and take them into account while computing centrality measures. The applied discretization, detailed in Section 3.4., consists in grouping similar weights with intervals defined as follow: $[t, t + \alpha \cdot t]$. The weight discretization is analyzed for α varying from 0.1 to 0.3. Higher values are not realistic because they assume that a path whose travel time increased by almost half of the shortest one is perceived as equivalent by the driver. With the increase of shortest paths number (Fig. 4b), observed for α equal to 0.1 to 0.3, more possibilities exist to join two nodes regarding the BC definition. In traffic perspective, this implies that BC will capture the criticality of the possible taken paths by drivers rather than the topologically shortest one. We chose to allocate the mean values of corresponding interval to edges but it could also be done with the maximal one, which would only impact GE. The global metric would be lower with the same trend, because of the increase of travel time. Used paths are distributed over different roads for the same origin destination, reproducing the actual users behaviors.

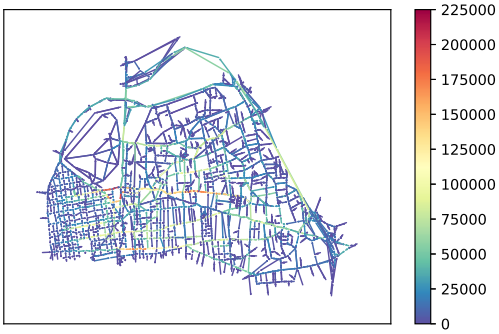

(a) Edge BC with "real" weights

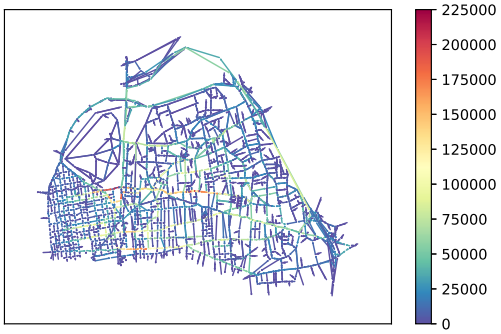

(b) Edge BC with discretized weights

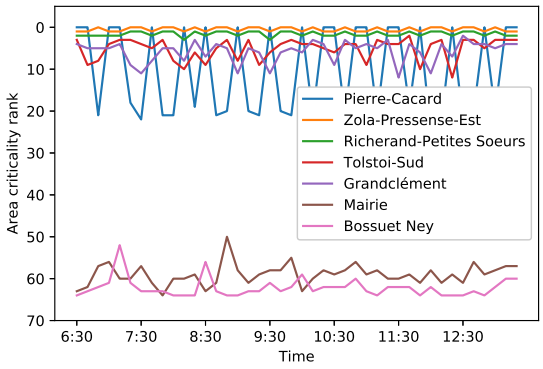

(c) Area criticality rank with "real" weights

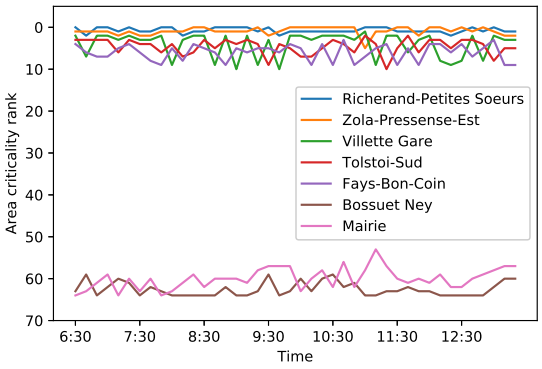

(d) Area criticality rank with discretized weights

Figure 5: Link distribution of BC over the network at 8:30am and rank of five originally most critical areas and two less ones according to their BC under normal conditions.

About centrality measures, at the global level, only slightly changes are visible, in case of discretized weights. Indeed, Fig. 4d and 4c present almost superimposed curves like the average paths travel time for all origins destinations (Fig. 4a). Nevertheless, we can observe that a small change in average shortest path travel time could have huge impact on GE (a peak is present at 10:40am for an α value equal to 0.1 and at the same time the average shortest path travel time is a bit reduced). The evolution of the weighted topological global metrics mostly depends of the vehicles number and not to their road usage.

At local scale (Fig. 5), the change in edges BC distribution at 8:30am is not really impacted (Fig. 5a and Fig. 5b). By ranking the five most critical areas and the two less critical ones in both weighting cases (Fig. 5c and Fig. 5d), we capture the discretization effect due to the new shortest path distribution. Some areas are thus crossed by these new paths, captured in the centrality measures, using the discretization. Nonetheless, in free flow conditions, the discretization does not have a big influence over the results.

4.3.3. Evolution of network performances with discretized weights in congested situation

To observe the impact of discretization in presence of congestion, we run a simulation from 6:30am to 1:30pm in presence of a blockage. At global level, we notice a continuously increase in the number of vehicles over the network (Fig. 6c. This implies a global decrease of performances (Fig.

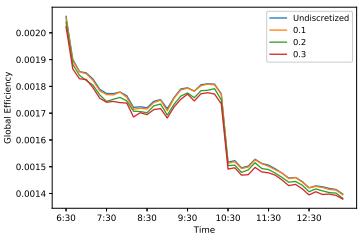

(a) Evolution of TTW GE

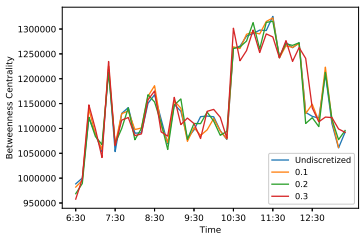

(b) Evolution of TTW GBC

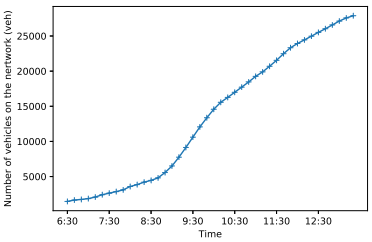

(c) Number of vehicles in the network

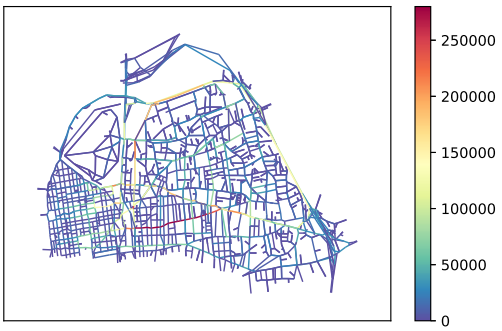

(d) Edge BC with "real" weights

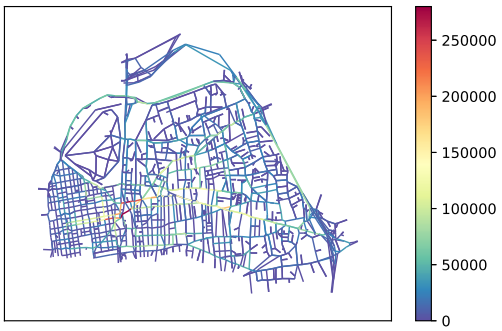

(e) Edge BC with discretized weights

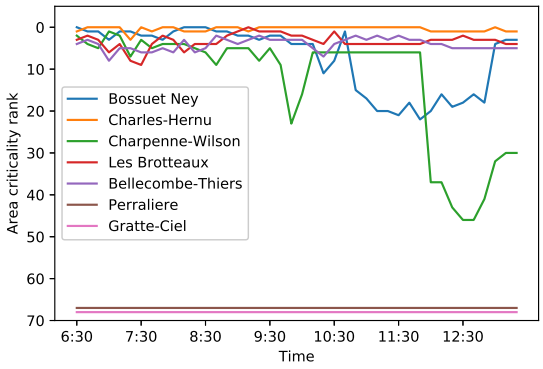

(f) Area criticality rank with "real" weights

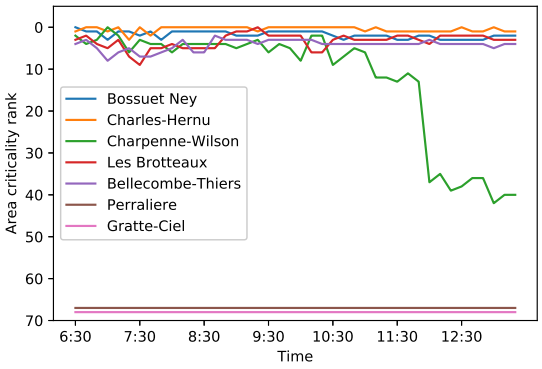

(g) Area criticality rank with discretized weights

Figure 6: Evolution of the graph-based weighted metrics between 6:30am and 1:30pm for discretized weights $[t, \alpha \cdot t]$ and different values of α in presence of congestion at global and edges BC distributions at 8:30am and area rankig at local levels.

6a and Fig. 6b) with the reduction of GE and the increased peaks of BC. Global results still does not change significantly with the discretization.

Nevertheless, at local scale, the distribution of edge BC is completely different at 8:30am. The various distributions of criticality are related to the different paths used without and with discretized weights. In the non-discretized weights case (Fig. 6d) some roads are distinguished by their BC value as the ring road. When weights are discretized (Fig. 6e) BC is slightly better distributed over the network, although we see a group of critical links close to the center of the network. The ranking of the five originally most critical areas and the two less ones over time, are realized with (Fig. 6g)

and without (Fig. 6f) discretized weights. With the second weighting option, positions of areas in ranking are more stable. This is the result of the better distribution in road usages. The increase of travel over a link is mostly absorbed by its equivalent paths. It does not always imply a change in path, like for the non-discretized scenario. In both cases, the rank of "Charpennes", represented in green, declines. At 10:30am, contained links begin to clog up. The shortest paths change and pass through new areas. Its BC decreases, causing an important rank fall from 10:30am to the end of the simulation. As it corresponds to the appearance of a strong and sustained congestion, this area requires a particular attention. On the contrary, lowest-ranked areas, which conserve their positions in the rank from 6:30am to 1:30pm. Because they are constitute of links with long travel time or because they are outermost than other areas, they are less crossed and thus less critical.

4.4. Impact of the discretization of weights

At global scale (GBC and GE),the discretization of weights does not impact results a lot. The evolution of both metrics follow the same trend in both weighting methods. As the BC is dependent on the shortest paths number and composition, by increasing them via our discretization method, redundant shortest paths exist for a same itinerary and therefore more links are crossed. The criticality is thus spread over travel-time-equivalent redundant paths, modifying results. The major impact of this step is underlined by results issued from congested simulation where edges and ares BC distributions are completely modified (Fig. 6). From the rank analysis (Fig. 5d and Fig. 6g) we can extract some lines to manage transport network. An area with a rank almost constant proves that they are "insensitive" to traffic conditions and thus have not to be monitored as a priority, whereas a fall in ranking for a part of the network is due to its congestion, therefore it is a critical part. It is related to an increase of another part which becomes crossed by shortest paths. By reproducing the use of road network by adapting edge weights, we are able to quantify network resilience in relation to both its topology and its traffic conditions. It is essential to reliably reproduce network usages for an accurate resilience analysis regarding the significant change in BC distribution.

4.5. Comparison between area disruptions and link failure

In this part, we compare the consequences of area-wide disruption with the average impact caused by the successive links disturbances. We use a graph with free flow travel time discretized weights with an α value of 0.2. Our stress tests here consist in a reduction of capacity from 20% to 80% of initial conditions. In the first case, (Fig. 7a and Fig. 7c), all links contained in the central area (Fig.1) are disturbed simultaneously by a speed reduction and thus a diminished capacity. In the second case (Fig. 7b and Fig. 7d), same links are disturbed successively. The results are averaged.

Regarding GE (Fig. 7f), the decreasing shape of network performances with respect of the capacity reduction is similar for both scenarios. When the capacity is disrupted and thus the speed is reduced, shortest paths travel time becomes longer by using bypass roads. By averaging the impacts of disturbance over successive links, global network performances are lower reduced than the area-wide disruption case. In the first case, the bypass consists in avoiding a unique link whereas in the second case, it has to circumvent an entire area. The new used path is longer in case of area-wide disruption, hence the greater loss of performances in term of GE.

To analyze the impact with BC, we focus on a capacity reduction of 60%. The results, by area, show different impacts (Fig. 7e) according to area-wide disruption (Fig. 7c) and successive link ones (Fig. 7d). Nearby sectors are greatly impacted by the used simulation of disruption contrary to the surrounding ones. Indeed, these zones are too far to be crossed by the new shortest paths. Conversely to southern areas, BC is higher in case of area-wide disruption than for link failures in the north. This is due to the existence of a bypass road for the impacted portion of "Cours

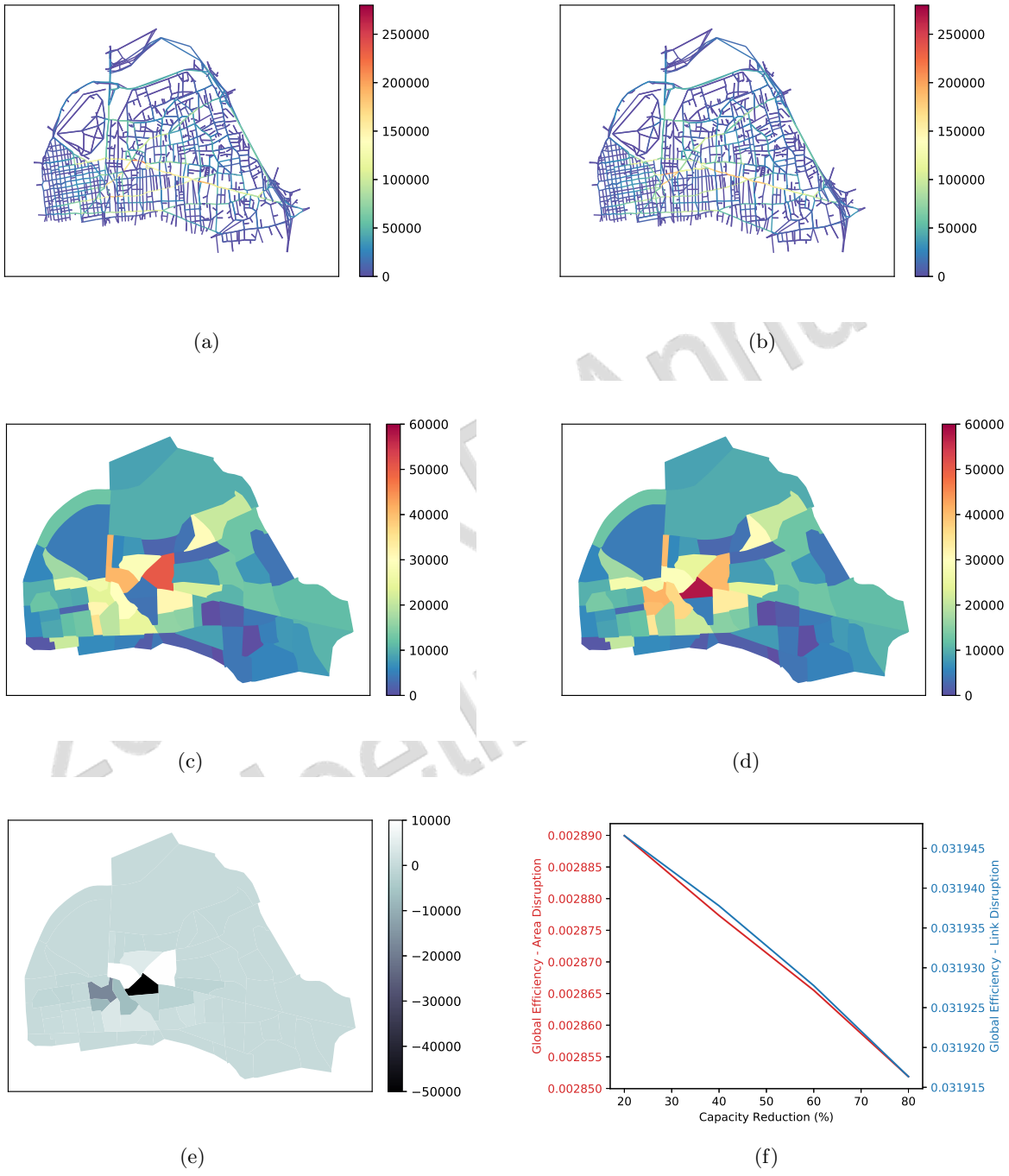

Figure 7: Results for simulation of disruption over an area by diminishing all capacity link (a) (c) or averaged results of one link capacity reduction for all contained in the area (b) (d). Differences are presented in (e) by subtracting the mean successive link disruption impacts of area-wide disruption one. Impact of these different disruptions is computed by GE on (f). In both cases, capacity during the perturbation is equal to 40% of the one under normal conditions.

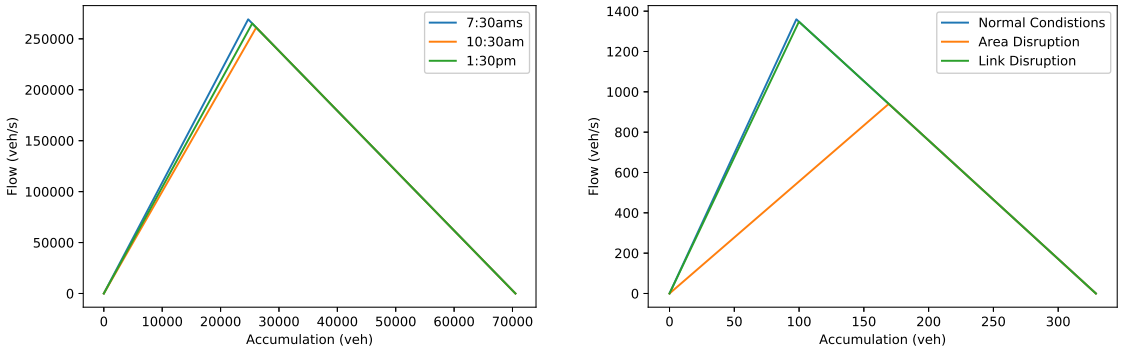

(a) MFD of the whole network at different hour

(b) MFD of the disturbed area

Figure 8: Macroscopic Fundamental Diagrams (MFD)

Emile Zola" when the whole sector is disturbed (Fig. 7a). In that situation, there is no shortest path passing through this sector, reducing its BC to almost zero. All links capacity is reduced simultaneously, deleting possible redundant paths inside the disturbed area. With successive link failures, some edges located in the disturbed area, still present a travel time benefit and therefore crossed by shortest paths (Fig. 7b). These results prove the importance to focus also on area-wide disruption in resilience analysis.

4.6. Traffic indicators

4.6.1. Evolution in time

To observe the evolution of global networks characteristics at different time, we plot the MFD of the whole studied network in congested situation (Fig. 8a).

The network capacity is the highest at 7:30am. At this time, only few vehicles are presented over the network (Fig. 3d) which operates under normal and optimal conditions. The major decrease of global capacity is observed at 10:30am. The drop of capacity is about $4000veh/s$. This is related to the increase of the GBC (Fig.3b) and the decrease of GE (Fig.3a). By increasing the number of vehicles over the network, several roads become congested, reducing their speed. The maximal capacity is reduced, impacted the MFD shape and used paths are distributed over longer ones, transiting over more links.

Finally, at the end of the simulation time, at 1:30pm, maximal capacity is slightly improved. Network regains a part of these initial conditions. This is also the case for centrality measures.

4.6.2. Comparison of disruption methods

To compare results of disruptions methods we plot the MFD of the disturbed area (Fig. 1b). The results (Fig. 8b) are obtained under normal conditions (blue curve), with the average impact of successive reduction of link capacity (orange curve) and when their capacity are reduced simultaneously (green curve). The disruption consists in a reduction of 60% of the initial capacity.

Area-wide disruption impact is more important than for the average of the successive links failures impacts. The maximal capacity is reduced about $400veh/s$. Although the consequences were greater with the resilience metrics, the trend is identical. The successive link failure method gives a MFD close to the one obtained under normal conditions (Fig. 8b). This was already the case for BC (Fig. 2f and Fig.7d).

4.6.3. Assessment

The centrality measures and the MFD are related. Indeed, a reduction of capacity implies a rise of travel time causing a change to longer shortest paths with a longer sequence of crossed links.

5. CONCLUSION AND PERSPECTIVES

In this work we propose contributions to network resilience modeling and analysis by improving classical topological metrics through the integration of traffic dynamics via a simulation-based approach. In addition, comparisons between those metrics and the MFD are performed.

By means of a dynamic weighted graph, we relate static and dynamic approaches. Outcomes present the heavy dependence of weights in topological metrics results. The choice of travel time weighting is motivated by the analysis lead in Section 4.2. By grouping similar travel time edges, reproducing accurately the users path choice, we obtain a new distribution of topological criticality, consistent with traffic conditions.

Regarding simulation of disruptions, area-wide ones have to be chosen to reproduce effect of some events like floods, social movement or power outage which impact several links over sectors. Reproduction of these impacts are not possible by link failures as shown in Fig. 7. This type of disruptions allows to study resilience of specific events. It could also be used to rank areas regarding their criticality.

Finally, relations between the traffic indicator and the metrics of resilience is demonstrated. An increase of BC is related to a decrease of the maximum flow in the MFD this is the ultimate goal as we expect that our newly developed resilience metrics to incorporate, in an accurate manner, traffic dynamics.

For future works, objective will be to characterize resilience of multimodal network. Thus, socio-economic information for studied area will highlight about favored transport mode and number of trip going from or arriving in a given area.

ACKNOWLEDGMENTS

This work has been supported by the French ANR project, PROMENADE, grant number ANR-18-CE22-0008.

AUTHOR CONTRIBUTION STATEMENT

The authors confirm contribution to the paper as follows: study, conception and design: EH, AF, NEEF; analysis and interpretation of results: EH, AF, NEEF; EH was the lead writer of the manuscript. All authors reviewed the results and approved the final version of the manuscript.

References

[1] Milan Janić. Reprint of "Modelling the resilience, friability and costs of an air transport network affected by a large-scale disruptive event". *Transportation Research Part A: Policy and Practice*, 2015.

[2] Erik Jenelius and Lars-Göran Mattsson. Road network vulnerability analysis of area-covering disruptions: A grid-based approach with case study. *Transportation Research Part A: Policy and Practice*, 46(5):746–760, 6 2012.

[3] Carlos F. Daganzo and Nikolas Geroliminis. An analytical approximation for the macroscopic fundamental diagram of urban traffic. *Transportation Research Part B: Methodological*, 42(9):771–781, 2008.

[4] Beth Doll and Mark A. Lyon. Risk and resilience: Implications for the delivery of educational and mental health services in schools. *School Psychology Review*, 27(3):348–363, 1998.

[5] Crawford S. Holling. Resilience of ecological systems. *Source: Annual Review of Ecology and Systematics*, 4:1–23, 1973.

[6] James P. G. Sterbenz, David Hutchison, Egemen K. Çetinkaya, Abdul Jabbar, Justin P. Rohrer, Marcus Schöller, and Paul Smith. Resilience and survivability in communication networks: Strategies, principles, and survey of disciplines. *Computer Networks*, 54:1245–1265, 2010.

[7] Michel Bruneau, Stephanie E. Chang, Ronald T. Eguchi, George C. Lee, Thomas D. O 'Rourke, Andrei M. Reinhorn, Masanobu Shinozuka, Kathleen Tierney, William A. Wallace, and Detlof Von Winterfeldt. A Framework to Quantitatively Assess and Enhance the Seismic Resilience of Communities. *Earthquake spectra*, 19:733–752, 2003.

[8] Alfred R. Berkeley and Mike Wallace. A Framework for Establishing Critical Infrastructure Resilience Goals Final Report and Recommendations by the Council. *National Infrastructure Advisory Council*, 2010.

[9] Lars Göran Mattsson and Erik Jenelius. Vulnerability and resilience of transport systems - A discussion of recent research. *Transportation Research Part A: Policy and Practice*, 2015.

[10] Reuven Cohen, Keren Erez, Daniel ben Avraham, and Shlomo Havlin. Resilience of the Internet to Random Breakdowns. *Physical Review Letters*, 85(21):4626–4628, 2000.

[11] Amer Shalaby, P Eng, and David King. Performance Metrics and Analysis of Transit Network Resilience in Toronto. *Transport Research Board*, 2016.

[12] Pauline Gauthier, Angelo Furno, and Nour-Eddin El Faouzi. Road network resilience: how to identify critical linkssubject to day-to-day disruptions? *Transport Research Record*, 2018.

[13] Sybil Derrible. Network Centrality of Metro Systems. *PLoS ONE*, 7(7):e40575, 2012.

[14] Xiaodong Zhang, Elise Miller-Hooks, and Kevin Denny. Assessing the role of network topology in transportation network resilience. *Journal of Transport Geography*, 46:35–45, 6 2015.

[15] Zhang, Yuanyuan, Wang Xuesong, Zeng Peng, and Xiaohong Chen. Centrality characteristics of road network patterns of traffic analysis zones. *Transport Research Record*, 2011.

[16] Freeman Linton C. A set of measures of centrality based on betweenness. *Sociometry*, pages 35–41, 1977.

[17] Angelo Furno, Nour-Eddin El Faouzi, Rajesh Sharma, and Eugenio Zimeo. Fast Computation of Betweenness Centrality to Locate Vulnerabilities in Very Large Road Networks. *Transport Research Board*, 2018.

[18] Meisam Akbarzadeh, Soroush Memarmontazerin, Sybil Derrible, and Sayed Farzin Salehi Reihani. The role of travel demand and network centrality on the connectivity and resilience of an urban street system. *Transportation*, pages 1–15, 8 2017.

[19] Vito Latora and Massimo Marchiori. Efficient Behavior of Small-World Networks. *Physic Review*, 87(89), 2001.

[20] Michal Bíl, Rostislav Vodák, Jan Kubeček, Martina Bílová, and Jiří Sedoník. Evaluating road network damage caused by natural disasters in the Czech Republic between 1997 and 2010. *Transportation Research Part A: Policy and Practice*, 80:90–103, 10 2015.

[21] Nazli Yonca Aydin, Hans Rudolf Heinimann, H Sebmen Duzgun, and Friedemann Wenzel. Integration of stress testing with graph theory to assess the resilience of urban road networks under seismic hazards. *Natural Hazards*, 91:37–68, 2018.

[22] Yingying Duan and Feng Lu. Robustness of city road networks at different granularities. *Physica A: Statistical Mechanics and its Applications*, 2014.

[23] Paolo Crucitti, Vito Latora, and Sergio Porta. Centrality Measures in Spatial Networks of Urban Streets. Technical report, 2005.

[24] Yaniv Altshuler, Rami Puzis, Yuval Elovici, Shlomo Bekhor, and Alex Pentland. Augmented Betweenness Centrality for Mobility Prediction in Transportation Networks. 2011.

[25] Rami Puzis, Yaniv Altshuler, Yuval Elovici, Shlomo Bekhor, Yoram Shiftan, and Alex Pentland. Augmented betweenness centrality for environmentally aware traffic monitoring in transportation networks. *Journal of Intelligent Transportation Systems: Technology, Planning, and Operations*, 2013.

[26] Vicenzo Nicosia, John Tang, Cecilio Mascolo, Mirco Musolesi, Giovanni Russo, and Vito Latora. *Temporal Networks*. 2013.

[27] Yew-Yih Cheng, Roy Ka-Wei Lee, Ee-Peng Lim, and Feida Zhu. DelayFlow centrality for identifying critical nodes in transportation networks. In *Proceedings of the 2013 IEEE/ACM International Conference on Advances in Social Networks Analysis and Mining - ASONAM '13*, 2013.

[28] Yew-Yih Cheng, Roy Ka, Wei Lee, Ee-Peng Lim, and Feida Zhu. Measuring Centralities for Transportation Networks Beyond Structures. *Lecture Notes in Social Networks*, 2015.

[29] Suhyung Yoo and Hwasoo Yeo. Evaluation of the resilience of air transportation network with adaptive capacity. *International Journal of Urban Sciences*, 2016.

[30] Pamela Murray-Tuite. A comparison of transportation network resilience under simulated System Optimum and User Equilibrium conditions. *Proceedings of the 2006 Winter Simulation Conference*, 2006.

[31] Eduardo Leal de Oliveira, Licínio da Silva Portugal, and Walter Porto Junior. Determining Critical Links in a Road Network: Vulnerability and Congestion Indicators. *Procedia - Social and Behavioral Sciences*, 162:158–167, 12 2014.

[32] Erik Jenelius, Tom Petersen, and Lars-Göran Mattsson. Importance and exposure in road network vulnerability analysis. *Transportation Research Part A*, pages 537–560, 2006.

[33] Juan Carlos Lam, Bryan T. Adey, Magnus Heitzler, Jürgen Hackl, Pierre Gehl, Noel van Erp, Dina D'Ayala, Pieter van Gelder, and Lorenz Hurni. Stress tests for a road network using fragility functions and functional capacity loss functions. *Reliability Engineering & System Safety*, 173:78–93, 2018.

[34] Susana Freiria, Bernardete Ribeiro, and Alexandre O. Tavares. Understanding road network dynamics: Link-based topological patterns. *Journal of Transport Geography*, 46:55–66, 6 2015.

[35] B Berche, C Von Ferber, T Holovatch, and Yu Holovatch. Resilience of public transport networks against attacks. *Eur. Phys. J. B*, 71:125–137, 2009.

[36] Sunghoon Kim and Hwasoo Yeo. A Flow-based Vulnerability Measure for the Resilience of Urban Road Network. *Procedia - Social and Behavioral Sciences*, 2016.

[37] Pin-Yu Chen and Alfred O Hero Iii. Node Removal Vulnerability of the Largest Component of a Network. *IEEE GlobalSIP*, 2013.

[38] Xiaoyu Qian. Application of Macroscopic Fundamental Diagrams to Dynamic Traffic Management. Technical report, 2009.

[39] Gerd Gigerenzer and Reinhard Selten. *Bounded rationality : the adaptive toolbox*. MIT Press, 2001.

[40] Michael Sivak. How common sense fails us on the road: contribution of bounded rationality to the annual worldwide toll of one million traffic fatalities. *Transportation Research Part F: Traffic Psychology and Behaviour*, 5(4):259–269, 2002.

[41] Edsger W. Dijkstra. *A short introduction to the art of programing*. 1971.

[42] M J Lighthill and G B Whitham. On kinematic waves II. A theory of traffic flow on long crowded roads. Technical report.

[43] Paul I. Richards. Shock Waves on the Highway. *Operations Research*, 4(1):42–51, 2 1956.

[44] Aric A. Hagberg, Daniel A. Schult, and Pieter J. Swart. Exploring Network Structure, Dynamics, and Function using NetworkX. In *Proceedings of the 7th Python in Science Conference (SciPy 2008)*, 2008.